Viser Technology Pte. Ltd.
Mechanical Engineering Science
DOI: 10.33142/mes.v4i1.7516

Research Article Open Access

A Novel Dual Helical Magnetorheological Fluid Micro-Robot

Zhixiang LI[1], Minglu CHI[1*], Shuaibing CHANG[2], Xiaoyan QIAN[3], Jiawen JIA[1], Jianbo LI[1], Chenyu WANG[1], Zuhua GUO[4]

1 School of Intelligent Engineering, Henan Institute of Technology, Henan Xinxiang 453000, China
2 School of Electrical Engineering and Automation, Henan Institute of Technology, Henan Xinxiang 453000, China
3 School of Economics, Henan Institute of Technology, Henan Xinxiang 453000, China
4 College of Computer Science and Technology, Henan Institute of Technology, Henan Xinxiang 453000, China

***Corresponding Author:** Minglu CHI, School of Intelligent Engineering, Henan Institute of Technology, Xinxiang, Henan, China; cmlcml86@163.com*

Abstract:
To address the problem of flexible drive control of gastrointestinal (GI) tract micro-capsule robot posture, a novel dual helix magnetorheological fluid (MRF) micro-robot (DHMRFMR) is proposed and developed in this paper. Based on the mechanical properties of magnetorheological fluid, the relationship model of magnetic field force is obtained, and the thrust model is established. Double micro DC deceleration motor is used to drive the two ends of the helical actuator to make the DHMRFMR forward and backward, by changing the external magnetic field rotation speed, direction and distance, adjust the attitude direction of the robot. Numerical simulation software ANSYS is used to analyze the motion law of external fluid of DHMRFMR, and the visualization of fluid velocity and pressure distribution is realized. The front-end helix actuator can change the flow path of the fluid, and the middle and tail of the DHMRFMR bear less pressure, which improves the stability and flexibility of the robot. The novel DHMRFMR is suitable for internal drive in bending environment, and has a good application prospect in biomedical engineering field in human intestinal unstructured environment.

***Keywords:** Dual helical actuation; Micro-robot; Magnetorheological fluid; Attitude control; Simulated analysis*

Introduction

GI tract diseases are not only prevalent in the elderly, but also in an increasing number of young people. High-risk groups need to be examined every 1-2 years, which poses severe challenges to the screening and treatment of GI tract diseases [1]. Traditional interventional gastroscopy is painful and risky, requiring patients to endure great pain. The birth of capsule endoscope greatly saves the manpower and time of GI tract disease diagnosis [2]. A capsule is swallowed with water and the whole digestive tract is traversed with gastrointestinal peristalsis without intubation. Doctors diagnose diseases on the external receiving display according to the pictures or videos taken by the capsule endoscope [3]. Compared with traditional gastroscopy, it can effectively avoid cross infection during examination in addition to eliminating the pain caused by intubation.

At present, the passive capsule robot that relies on intestinal peristalsis for GI examination has the following problems: (i) Passive capsule robots move slowly and can only move forward. (ii) The passive capsule robot is unable to stop at a problematic lesion, let alone return for a re-examination. (iii) Passive capsule robots mostly use

batteries to power their cameras. Fixed and long time shooting can produce a lot of non-diagnostic photos and waste storage space. (iv) The passive capsule robot takes a long time to check, resulting in low inspection efficiency and the possibility of missing detection [4]. Therefore, the active capsule robot came into being, can take the initiative to explore and diagnose, greatly improve the efficiency of diagnosis and treatment. The active capsule robot can reside in a suspected patient area for observation or sampling, and has various functions of active control and can interact with the doctor. In the past decade, several locomotion mechanisms were developed to provide active propulsion for capsule endoscopes, including the rotating spiral [5], inchworm-like [6], legged [7], paddle-based [8] and vibro-impact locomotion mechanisms [9].

At present, the active capsule robot is mainly divided into two ways: electric energy drive and magnetic energy drive. Tabak et al. [10] proposed a bionic

Received on April 20, 2022; Accepted on May 10, 2022

capsule robot based on the movement principle of eukaryotic microorganisms, and controlled the capsule robot to complete multi-directional movement by a spiral tail. Tortora et al. [11-12] developed a capsule robot driven by a four-screw motor, which was applied to the diagnosis in a wide range, such as the stomach. The capsule is equipped with a visual imaging system that allows doctors to see inside the stomach using an interactive system. Norton et al. [13] proposed a wheeled micro-robot with expansion and contraction function for colon examination. Park et al. [14] developed a inchworm-like capsule to achieve forward movement through the pulling of the outrigger.

Because magnetic energy has the advantage of efficient transmission, it can not only realize wireless control, but also solve the problem of power endurance of the capsule robot. Therefore, applied magnetic field as the driving source of capsule robot has attracted extensive attention. Salerno et al. [15] proposed a "master-slave magnetic coupling" driving method for capsule robot, using a permanent magnet installed at the end of the manipulator as the main magnetic source. Through the magnetic coupling effect, the capsule robot with embedded permanent magnet will generate magnetic pull to achieve movement. Gumprecht et al. [16-17] developed a magnetic field drive device that uses electromagnets to apply magnetic force to the capsule robot to move and release drugs. Zhang et al. [18-19] studied the accuracy and feasibility of positioning and proposed a magnetic levitation system of magnetic levitation capsule robot, which controlled the steering and movement of the robot by the magnetic attraction or repulsion force generated. Qinyuan Shi et al. [20] propose an optical-magnetic fusion tracking framework to track the magnetically actuated capsule robot in real time. The proposed method utilizes the prior-known pose of external permanent magnet estimated from the optical tracking method to decouple internal permanent magnet's magnetic field from the composite magnetic field to achieve higher tracking accuracy of wireless capsule endoscopy. Puhua Tang et al. [21] designed and manufactured a set of drive systems for a capsule robot in a pipe driven by an external permanent magnet, and a measurement system of the fluid flow field in the pipe during the robot's precession.

In conclusion, regarding the operating performance of capsule robots, the existing research mainly focuses on the drive control of the capsule robot driven by electric energy or magnetic energy alone. However, the combination of electric drive and magnetic energy drive for attitude control has not been discussed. Moreover, none of the above studies considered the use of magnetorheological fluid as the magnet medium to achieve intelligent control. These unsolved issues are the motivation of our research work presented in this paper.

To overcome this problem and provide an effective attitude control method in unstructured GI tract, we have developed a novel DHMRFMR, and proposed a attitude drive control method of robot that combines electric drive and magnetic drive. The motion control of the DHMRFMR is realized by using a miniature DC reduction motor to control the front and rear helical actuator and magnetorheological fluid is used as attitude control medium. The thrust model and magnetic field force relationship model of the DHMRFMR are established, which can effectively control the attitude navigation of the robot. Finite element analysis software ANSYS is used to analyze the motion law of external fluid of DHMRFMR, and the visualization of fluid velocity and pressure distribution is realized. The results show that the front-end screw actuator can change the fluid flow path and make the middle and tail of the DHMRFMR bear less pressure. The motion stability of the DHMRFMR is improved, and it can move flexibly in the complex bending intestinal environment. This paper provides a basis for attitude control and navigation drive of micro-robot in unstructured environment.

1 Design of DHMRFMR Drive Control System

The core of the DHMRFMR drive control system is "drive" and "control" Through this system, the DHMRFMR can be controlled to move in the GI tract to achieve the purpose of stomach and intestinal examination. The overall design of DHMRFMR drive control system in this paper includes two parts: power system and pose control system. The whole control function of the DHMRFMR is shown in Figure 1.

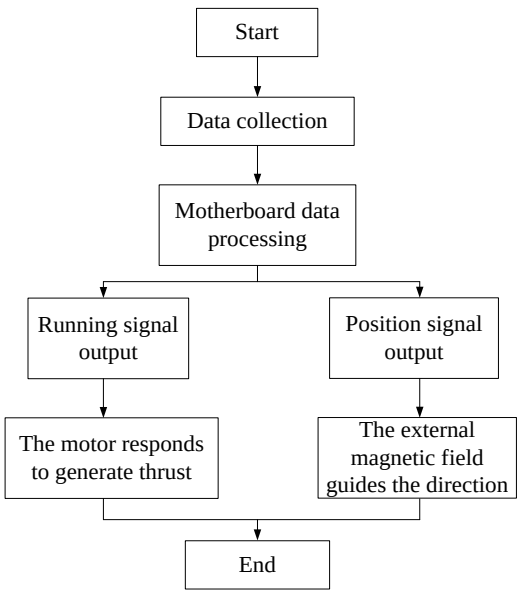

Figure 1 The whole control function of the DHMRFMR

The overall control process of the DHMRFMR is as

follows: When the DHMRFMR starts to work, a signal transmitter sends out a signal. The internal motor controller receives the signal through the signal receiver, and controls the rotation of the miniature DC reduction motor to drive the external dual helix actuator, which then generates counterthrust to push the DHMRFMR forward or backward. At the moment, the attitude control system starts the attitude adjustment function. Under the action of an external magnetic field, the magnetorheological fluid inside the DHMRFMR changes under the influence of the magnetic field, and gathers together to produce a certain force, which changes the direction of the DHMRFMR's movement. When the external magnetic field changes, the direction of action of the internal force will also change, thus changing the direction and attitude of the DHMRFMR movement.

1.1 Design of DHMRFMR Power System

Power system is mainly composed of miniature DC reduction motor, motor controller, signal receiver, signal transmitter, helix actuator and power supply, as shown in Figure 2. Due to the small size required by the medical capsule robot, there is a strict volume limitation for the power system, and the motor volume used is also small, and the performance thrust can meet the requirements. The precession device must also meet volume requirements.

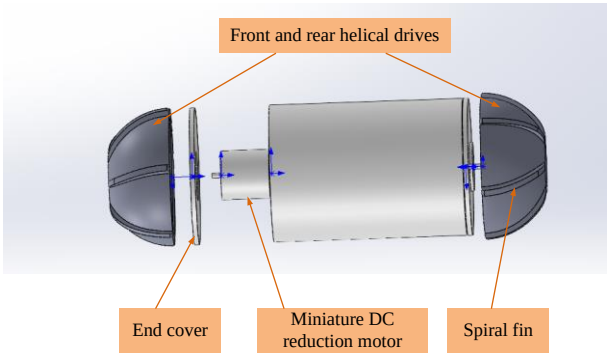

Figure 2 DHMRFMR integral structure

When the DHMRFMR enters the GI tract, the power system starts work. The external helical actuator is driven by the rotation of the motor, and the rib plate of the spiral rib will interact with the fluid in the GI tract to generate a force to push the DHMRFMR forward. The power system is driven by the front and rear dual drives, and the helical actuators at the front and rear ends of the DHMRFMR turn forward and reverse under the control of the miniature DC reduction motor. The DHMRFMR can move forward and backward without turning, which greatly improves the mobility of the robot in the GI tract.

1.2 Helical actuator Shape Design of Power System

The semicircular shape of the helical actuator can reduce the scratches on the GI tract wall during the rotation of the spiral ribs of the DHMRFMR, and reduce the resistance of the robot when moving in the liquid environment. The helical actuator is 3D printed with medical materials, which has the characteristics of corrosion resistance, good wear resistance and stable performance. The helical actuator is light in weight and stable in structure. The DHMRFMR helical actuator is shown in Figure 3.

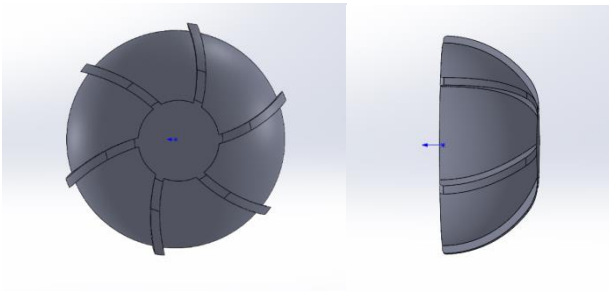

Figure 3 Helical drive for DHMRFMR

1.3 Miniature DC Reduction Motor for Dual Helix Power System

The DHMRFMR drive control power system uses two DC reduction motors to drive the front and rear helical actuators. The motor is easy to control, good stability, strong adaptability to the environment. The experiment is carried out in a transparent plexiglas tube, so the open-loop control method can meet the demand of speed control. The motor has a voltage range of 0.2-6 V, rated voltage of 3 V, maximum speed of 1200 r/min, current of 25 mA, and power of 0.1 W. The total length of motor is 16.5 mm, the diameter of reduction box is 6 mm, and the reduction ratio of reduction box is 1:26, as shown in Figure 4.

Figure 4 Miniature DC reduction motor

The power system adopts wireless remote control, which is composed of radio frequency transmitter and radio receiver. Wireless transmission adopts the point control mode. Press the button to turn forward, and press

the button again to reverse the motor, as shown in Figure 5. The wireless transmitter has small volume, low power consumption and wide voltage range. In standby state, the current is only 0.05 mA, and the working voltage is DC 3V. It has low energy consumption and can work for a long time.

The size of the wireless receiver is 21mm×11mm×5mm, the voltage range is DC 3V-12V, and the maximum current is 0.4 A. The receiver itself has overcurrent protection function. The black line is the negative pole of the power supply, the red line is the positive pole of the power supply, and the yellow line is the receiver's two outputs, controlling two DC reduction motors. The power supply is lithium battery with a size of 19mm×10mm×4mm and a voltage of 3.7 V, as shown in Figure 6.

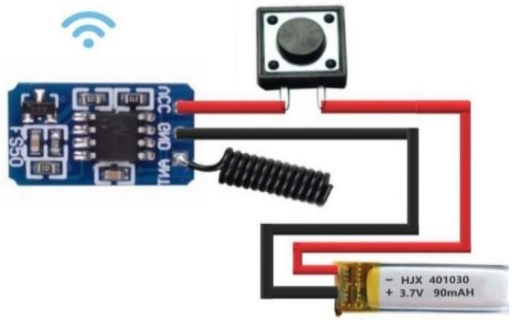

Figure 5 Wireless control transmitter

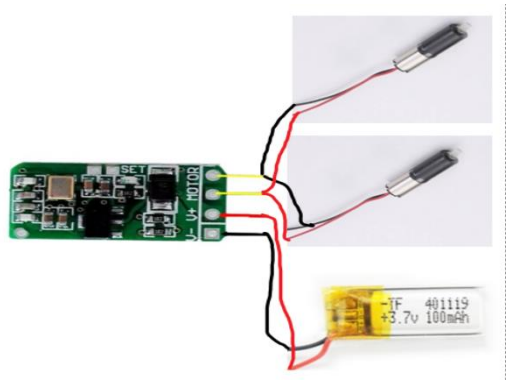

Figure 6 Wireless receiver

1.4 Analysis and Calculation of Helical Thrust Force of Power System

Microrobots move forward in a closed environment by pushing the fluid at the front with the helical head. The fluid will be obstructed in the reverse direction, and the fluid will enter the rear area along the side of the DHMRFMR. If the swimming speed of the DHMRFMR is high, the fluid on the surface is laminar flow, and the fluid stuck to the surface of the robot rotates synchronously with the robot. If the fluid does not pass quickly through the side of the DHMRFMR to the rear area, turbulent conditions can occur. The condition for satisfying Bernoulli's equation is that the fluid is in laminar flow state, which is the ideal state.

As the DHMRFMR spins forward, the fluid in front of it is separated by the robot and flows sideways. The DHMRFMR is subjected to axial fluid resistance, called frictional resistance Ff. The fluid has a certain viscosity, the part of the fluid near the DHMRFMR surface will speed up, forming a boundary layer on the surface. At this point, the fluid pressure on the front and back ends of the DHMRFMR is different, forming fluid resistance, known as differential pressure resistance Fc. The total resistance of the DHMRFMR is the sum of Ff and Fc, that is:

$$F_{to} = F_f + F_c \tag{1}$$

Frictional resistance and differential pressure resistance can be obtained by multiplying the kinetic energy of the flow per unit volume by a certain area, and then multiplying by the drag coefficient, can be expressed as

$$F_f = C_f \frac{\rho v^2}{2} S_f \tag{2}$$

$$F_c = C_p \frac{\rho v^2}{2} S_p \tag{3}$$

where *Cf* and *Cp* are the drag coefficients of friction resistance and differential pressure resistance respectively, *Sf* is the area under shear stress, *Sp* is the projected area of the object perpendicular to the direction of flow velocity, ρ is density, and v is the speed of the DHMRFMR. Therefore, the total resistance can be expressed as

$$F_{to} = C_D \frac{\rho v^2}{2} S \tag{4}$$

where *CD* is the total drag coefficient, S is the area projected against flow of the object in the vertical direction of flow velocity, so S=*Sp*. When the total driving force of the DHMRFMR is equal to the total fluid resistance, the total thrust of the DHMRFMR can be obtained.

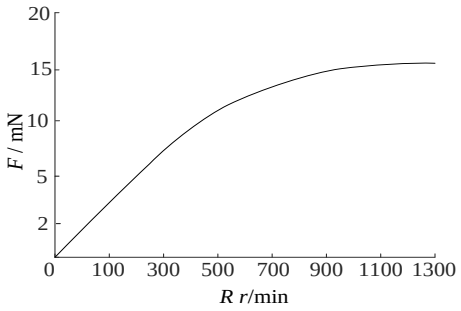

Figure 7 Diagram of helical thrust force changes with rotational speed

As shown in Figure 7, the helical thrust changes with the speed. With the increase of the speed of the miniature DC reducer motor of the power system, the helical thrust of the power system gradually increases. When the speed reaches 1000 r/min, the thrust is kept at about 15 mN, the speed continues to increase, and the

thrust is kept constant, indicating that the system has reached a dynamic equilibrium state at this time.

2 Pose Control System for DHMRFMR

The pose control system is used to adjust the pose direction of the DHMRFMR. Because the GI tract is an unstructured meandering environment, DHMRFMR needs to be able to change direction continuously during movement. DHMRFMR pose control is realized by coupling control of external magnetic field and internal magnet.

2.1 Fluid Mechanics Properties of MF

MF is a kind of intelligent fluid. The rheological properties of MF will change when there is a certain intensity of magnetic field in the environment, and it will change from a fluid to a solid with a certain viscoelasticity. If the magnetic field disappears, it will return from a solid with a certain viscoelasticity to the original liquid.

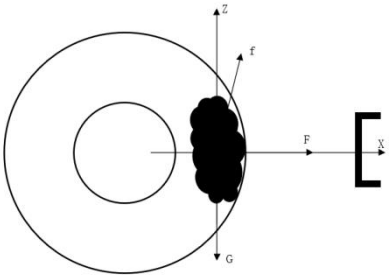

Figure 8 Force analysis of MF

According to this characteristic, the yield stress of the fluid can be controlled by changing the magnetic field intensity of the surrounding environment, so as to realize intelligent control of the magnetorheological fluid. The force on MF is shown in Figure 8. When the MF is in a certain magnetic field, the magnetic force is

$$F = \mu_0 V(M \cdot \nabla)H = V(M \cdot \nabla)B \tag{5}$$

where F is magnetic field force, $\mu 0$ is vacuum permeability, V is volume of MF, M is magnetization, ∇ is magnetic field gradient operator, H is magnetic field intensity, B is magnetic induction intensity. The magnetic induction intensity B and magnetization intensity M can be decomposed along X, Y and Z axes, which are Bx, By, Bz and Mx, My and Mz, respectively.

$$\begin{bmatrix} F_x \\ F_y \\ F_z \end{bmatrix} = V \begin{bmatrix} M_x \frac{\partial B_x}{\partial_x} + M_y \frac{\partial B_x}{\partial_y} + M_z \frac{\partial B_x}{\partial_z} \\ M_x \frac{\partial B_y}{\partial_x} + M_y \frac{\partial B_y}{\partial_y} + M_z \frac{\partial B_y}{\partial_z} \\ M_x \frac{\partial B_z}{\partial_x} + M_y \frac{\partial B_z}{\partial_y} + M_z \frac{\partial B_z}{\partial_z} \end{bmatrix} \tag{6}$$

2.2 Control Principle of Pose Control System

The pose control system mainly uses magnetic field environment composed of MF and external magnets to control the pose direction of the DHMRFMR. The shell of the DHMRFMR is a hollow cavity inside, which is used to contain MFs. When the DHMRFMR is placed in the magnetic field generated by the external magnetic field, the MF in the cavity is magnetized by the external magnetic field, which turns the originally uniformly distributed liquid into a concentrated spiky-shaped solid. The MF, which is concentrated together, creates a magnetic force under the action of a magnetic field, which changes the direction of motion of the DHMRFMR. By changing the distance and position between the external magnetic field and the internal MF, the position and attitude of the DHMRFMR can be changed.

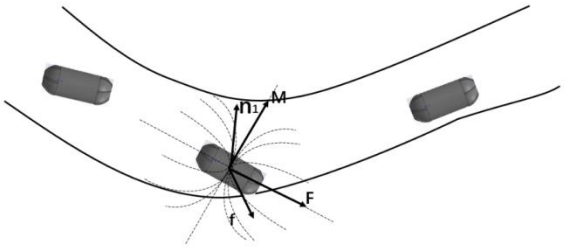

Figure 9 Attitude control diagram

Figure 9 is the attitude control diagram of the DHMRFMR. The dotted line represents the external magnetic field around the DHMRFMR. In Figure 8, the area with dense dotted line distribution indicates that the magnetic field intensity of the region is strong, while the area with sparse dotted line distribution indicates that the magnetic field intensity is weak. When the DHMRFMR is in the area with dense magnetic field lines, the MF inside the robot will be pushed and pulled more, and the direction of motion will change more easily.

3 Simulation Test Analysis of DHMRFMR System

To verify the correctness of the theoretical analysis and the feasibility of the device, the control system of DHMRFMR is developed. ANSYS 2021R1 software is used to simulate the velocity and pressure distribution of the DHMRFMR to realize the visualization of the flow field. Firstly, the model of driving motor and precession device is built by simulation software, and then the motor and precession device of the driving system are assembled and debugged, as shown in Figure 10. And finally the simulation is carried out by ANSYS software.

Figure 10 Attitude control diagram

The thrust, attitude and guidance of the DHMRFMR power device are tested, the value of thrust and the thrust adjustment of the power system under different working conditions are calculated by analyzing the simulated data, and the stability of the DHMRFMR under different thrust is analyzed. The structural parameters of the DHMRFMR are shown in Table 1.

Tab 1 Structural parameters of the DHMRFMR

Parameters	Notation	DHMRFMR
Length /(mm)	L	75
Diameter /(mm)	D	26
Mass /(g)	G	48.1
Helical actuator diameter (Maximum) /(mm)	Ds	27
Height of spiral ribs /(mm)	ka	1.2
Width of spiral groove (Maximum) /(mm)	N1	16
Width of spiral ribs /(mm)	N2	1.5
Helix angle /(°)	β	20
Working speed /(r/min)	n	1000

Before the simulation analysis, it is necessary to conduct 3D modeling of the DHMRFMR in Solidworks and 3D printing and manufacturing according to the 3D model. The 3D model and physical prototype are shown in Figure 11 (a) and Figure 11 (b), respectively.

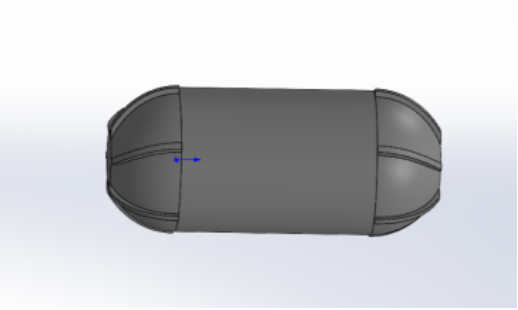

(a) 3D model of DHMRFMR

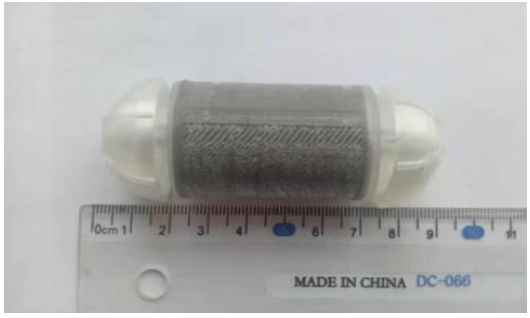

(b) Prototype of a DHMRFMR

Figure 11 Solidworks 3D model and prototype of DHMRFMR

The continuity equation and Navier-Stokes equation are regarded as the governing equations.

The continuity equation can be written as:

$$\frac{\partial(\rho u)}{\partial x}+\frac{\partial(\rho v)}{\partial y}+\frac{\partial(\rho w)}{\partial z}=0 \tag{7}$$

The Navier-Stokes equation can be expressed as:

$$\begin{cases}\dfrac{\partial(\rho u)}{\partial t}+div(\rho uU)=div(\mu gradu)-\dfrac{\partial p}{\partial x}+F_x\\ \dfrac{\partial(\rho v)}{\partial t}+div(\rho vU)=div(\mu gradv)-\dfrac{\partial p}{\partial y}+F_y\\ \dfrac{\partial(\rho w)}{\partial t}+div(\rho wU)=div(\mu gradw)-\dfrac{\partial p}{\partial z}+F_z\end{cases} \tag{8}$$

where u, v and w are the components of fluid velocity U on each coordinate axis, ρ and μ are the density and dynamic viscosity of fluid respectively, p is pressure, Fx, Fy and Fz are the mass force of fluid element on each coordinate axis.

The fluid in the pipeline is meshed and the DHMRFMR surface meshes are locally encrypted to improve the calculation accuracy. The fluid type is set as liquid, the dynamic viscosity is 1.0 Pa s, and the rotation axis of the DHMRFMR model is set as along the Y-axis. Establish the cloud picture of the operation interface, select the unit and data displayed on the operation interface, and start the simulation operation after checking the correctness.

When the DHMRFMR runs at a certain speed in the fluid, the velocity distribution cloud of the surrounding environment is shown in Figure 12. In the Figure, the external fluid moves with the DHMRFMR at the same time and has a follow-up effect. The farther away from the DHMRFMR, the lower the degree of fluid flow. At the far end, the fluid flow velocity is close to 0. This results in the fluid velocity on the surface being roughly the same as the DHMRFMR velocity. At the same time, it can be seen that the fluid velocity at the back end of the DHMRFMR is higher and has a greater driving force.

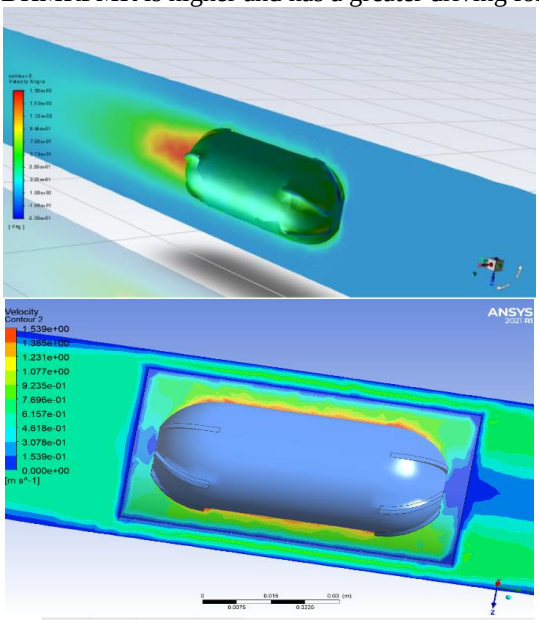

Figure 12 Cloud image of motion speed of DHMRFMR model

When the DHMRFMR runs, the ambient pressure of the liquid will change, and the helical actuator of the DHMRFMR model will also be subjected to a certain amount of fluid push back pressure. The pressure distribution cloud diagram generated by the operation is shown in Figure 13. In the Figure, the front-end of the DHMRFMR is subjected to a large fluid impact pressure, up to 274 Pa.

Because the pressure of the front-end helical actuator is larger, the fluid flow path is changed, and the middle and tail of the DHMRFMR bear less pressure, which improves the stability and flexibility of the DHMRFMR.

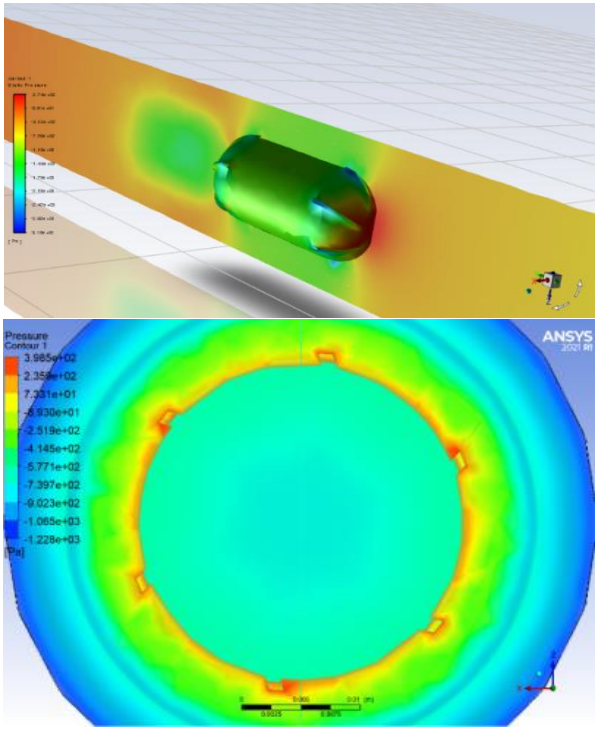

Figure 13 Pressure cloud diagram of DHMRFMR model

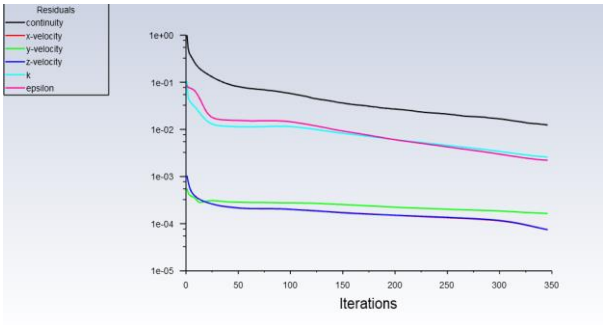

Figure 14 Floating point variation of simulation results

The simulation results show that the floating point variation of the DHMRFMR model is relatively stable. Floating point numbers do not generate large fluctuations, and there is no floating point overflow during operation. Floating point numbers form a relatively smooth curve, as shown in Figure 14. The operation results verify that the designed system is relatively stable and meets the design requirements.

4 Conclusions

In this paper, theoretical modeling and finite element simulation are carried out for important problems in attitude control of GI tract DHMRFMR. The simulation results are in good agreement with theoretical analysis. The main conclusions are as follows:

(1) A novel DHMRFMR is designed and developed, which consists of a miniature DC reduction motor, a motor controller, a signal receiver, a signal transmitter, a helical actuator, a MF cavity and a power supply. The DHMRFMR can move forward and backward without turning, with good movement flexibility.

(2) The DHMRFMR drive control system consists of pose control system and power system. The magnetic field force relationship model of MF is obtained and the thrust model is established. The pose control of DHMRFMR is realized by coupling control of external magnetic field and internal magnet. By changing the distance and position between the external magnetic field and the internal MF, the position and attitude direction of the DHMRFMR in the process of motion can be realized.

(3) Finite element analysis software ANSYS is utilized to analyze the external fluid movement law of DHMRFMR, and the visualization of fluid velocity and pressure distribution is realized. When the DHMRFMR moves in a fluid at a certain speed, the surrounding fluid moves simultaneously. Further away from the DHMRFMR, the flow velocity of the fluid is almost stationary. The front-end helical actuator can change the flow path of the fluid and improve the stability and flexibility of the DHMRFMR.

The breakthrough in the driving and control technology of the novel DHMRFMR has laid a clinical foundation for diagnosis and treatment and targeted drug delivery in the unstructured environment of human GI tract, and has a good application prospect.

Conflict of Interest

Te author declare that there is no conflict of interest regarding the publication of this paper.

Acknowledgement

This work was supported by the Key Research Development and Promotion Special Project of Henan Province, under Grant 212102310119 and 212102210358, Scientific Research Foundation for High-level Talents of Henan Institute of Technology, under Grant KQ1869, Research and Practice Project of Higher Education Teaching Reform in Henan Province, under Grant 2021SJGLX289, University-Industry Collaborative Education Program, under Grant 202101187010 and

202102120046, Innovation and Entrepreneurship Training Program for College Students of Henan Province, under Grant 202211329011, Educational and Teaching Reform Research and Practice Project of Henan Institute of Technology, under Grant 2021-YB023 and JJXY-2021005, Innovative Education Curriculum Construction Project of Henan Institute of Technology, under Grant CX-2021-005, 2022 Xinxiang Federation of Social Sciences Research topic, under Grant SKL-2022-254 and SKL-2022-228, 2022 Annual Research Topic of Henan Federation of Social Sciences, under Grant SKL-2022-2692.

References

[1] Bray F, Ferlay J, Soerjomataram I, et al, 2018. Global cancer statistics 2018: GLOBOCAN estimates of incidence and mortality worldwide for 36 cancers in 185 countries. CA: a cancer journal for clinicians, 68(6): 394-424.

[2] Rondonotti E, Spada C, Adler S, et al, 2018. Small-bowel capsule endoscopy and device-assisted enteroscopy for diagnosis and treatment of small-bowel disorders: European Society of Gastrointestinal Endoscopy (ESGE) Technical Review. Endoscopy, 50(4): 423-446.

[3] Bouchard S, Ibrahim M, Van Gossum A, 2014. Video capsule endoscopy: perspectives of a revolutionary technique. World Journal of Gastroenterology: WJG, 20(46): 17330.

[4] Slawinski P R, Obstein K L, Valdastri P, 2015. Capsule endoscopy of the future: What's on the horizon. World journal of gastroenterology: WJG, 21(37): 10528.

[5] Sendoh M, Ishiyama K, Arai K I, 2003. Fabrication of magnetic actuator for use in a capsule endoscope. IEEE Transactions on Magnetics, 39(5): 3232-3234.

[6] Kim B, Park S, Park J O, 2009. Microrobots for a capsule endoscope. IEEE/ASME International Conference on Advanced Intelligent Mechatronics. IEEE: 729-734.

[7] Quirini M, Menciassi A, Scapellato S, et al, 2008. Design and fabrication of a motor legged capsule for the active exploration of the gastrointestinal tract. IEEE/ASME transactions on mechatronics, 13(2): 169-179.

[8] Park H, Park S, Yoon E, et al, 2007. Paddling based microrobot for capsule endoscopes. Proceedings 2007 IEEE International Conference on Robotics and Automation. IEEE, : 3377-3382.

[9] Liu Y, Wiercigroch M, Pavlovskaia E, et al, 2013. Modelling of a vibro-impact capsule system. International Journal of Mechanical Sciences, 66: 2-11.

[10] Tabak A F, Yesilyurt S, 2012. Experiments on in-channel swimming of an untethered biomimetic robot with different helical tails. 4th IEEE RAS & EMBS International Conference on Biomedical Robotics and Biomechatronics (BioRob). IEEE: 556-561.

[11] De Falco I., Tortora G, Dario P., et al, 2014. An integrated system for wireless capsule endoscopy in a liquid-distended stomach. IEEE Transactions on Biomedical Engineering, 61(3):794-804.

[12] Tortora G., Valdastri P., Susilo E., et al, 2009. Propeller-based wireless device for active capsular endoscopy in the gastric district. Minimally Invasive Therapy & Allied Technologies, 18(5):280-290.

[13] Norton J, Hood A, Neville A, et al, 2016. RollerBall: a mobile robot for intraluminal locomotion. 6th IEEE International Conference on Biomedical Robotics and Biomechatronics (BioRob). IEEE: 254-259.

[14] Park H J, Kim D, Kim B, 2012. A robotic colonoscope with long stroke and reliable leg clamping. International Journal of Precision Engineering & Manufacturing, 13(8):1461-1466.

[15] Salerno M, Rizzo R, Sinibaldi E, et al, 2013. Force calculation for localized magnetic driven capsule endoscopes. IEEE International Conference on Robotics and Automation. IEEE: 5354-5359.

[16] Gumprecht J D J, Lueth T C, Khamesee M B, 2013. Navigation of a robotic capsule endoscope with a novel ultrasound tracking system. Microsystem technologies, 19(9): 1415-1423.

[17] Hosseini S., Mehrtash M, Khamesee M, 2011. Design, fabrication and control of a magnetic capsule-robot for the human esophagus. Microsystem Technologies, 17(5-7): 1145-1152.

[18] Zhang X, Mehrtash M, Khamesee M, 2016. Dual-axial motion control of a magnetic levitation system using hall-effect sensors. IEEE/ASME Transactions on Mechatronics, 21(2): 1129-1139.

[19] Mehrtash M, Khamesee M, Tsuda N., et al, 2012. Motion control of a magnetically levitated microrobot using magnetic flux measurement. Microsystem Technologies, 18(9-10): 1417-1424.

[20] Shi Q, Liu T, Song S, et al, 2021. An optically aided magnetic tracking approach for magnetically actuated capsule robot. IEEE Transactions on Instrumentation and Measurement, 70: 1-9.

[21] Tang P, Liang L, Guo Z, et al, 2021. Orthogonal optimal design of multiple parameters of a magnetically controlled capsule robot. Micromachines, 12(7): 802.